Artificial Intelligence–Powered Spatial Analysis of Tumor-Infiltrating Lymphocytes as Complementary Biomarker for Immune Checkpoint Inhibition in Non–Small-Cell Lung Cancer

Sehhoon Park, MD, PhD[1]; Chan-Young Ock, MD, PhD[2]; Hyojin Kim, MD, PhD[3]; Sergio Pereira, PhD[2]; Seonwook Park, PhD[2]; Minuk Ma, MS[2]; Sangjoon Choi, MD[4]; Seokhwi Kim, MD, PhD[5]; Seunghwan Shin, MD[2]; Brian Jaehong Aum, PhD[2]; Kyunghyun Paeng, MS[2]; Donggeun Yoo, PhD[2]; Hongui Cha, PhD[1]; Sunyoung Park, PhD[1]; Koung Jin Suh, MD[6]; Hyun Ae Jung, MD, PhD[1]; Se Hyun Kim, MD, PhD[6]; Yu Jung Kim, MD, PhD[6]; Jong-Mu Sun, MD, PhD[1]; Jin-Haeng Chung, MD, PhD[3]; Jin Seok Ahn, MD, PhD[1]; Myung-Ju Ahn, MD, PhD[1]; Jong Seok Lee, MD, PhD[6]; Keunchil Park, MD, PhD[1]; Sang Yong Song, MD, PhD[4]; Yung-Jue Bang, MD, PhD[7]; Yoon-La Choi, MD, PhD[4]; Tony S. Mok, MD[8]; and Se-Hoon Lee, MD, PhD[1,9]

PURPOSE Biomarkers on the basis of tumor-infiltrating lymphocytes (TIL) are potentially valuable in predicting the effectiveness of immune checkpoint inhibitors (ICI). However, clinical application remains challenging because of methodologic limitations and laborious process involved in spatial analysis of TIL distribution in whole-slide images (WSI).

METHODS We have developed an artificial intelligence (AI)–powered WSI analyzer of TIL in the tumor microenvironment that can define three immune phenotypes (IPs): inflamed, immune-excluded, and immune-desert. These IPs were correlated with tumor response to ICI and survival in two independent cohorts of patients with advanced non–small-cell lung cancer (NSCLC).

RESULTS Inflamed IP correlated with enrichment in local immune cytolytic activity, higher response rate, and prolonged progression-free survival compared with patients with immune-excluded or immune-desert phenotypes. At the WSI level, there was significant positive correlation between tumor proportion score (TPS) as determined by the AI model and control TPS analyzed by pathologists ($P < .001$). Overall, 44.0% of tumors were inflamed, 37.1% were immune-excluded, and 18.9% were immune-desert. Incidence of inflamed IP in patients with programmed death ligand-1 TPS at $< 1\%$, 1%-49%, and $\geq 50\%$ was 31.7%, 42.5%, and 56.8%, respectively. Median progression-free survival and overall survival were, respectively, 4.1 months and 24.8 months with inflamed IP, 2.2 months and 14.0 months with immune-excluded IP, and 2.4 months and 10.6 months with immune-desert IP.

CONCLUSION The AI-powered spatial analysis of TIL correlated with tumor response and progression-free survival of ICI in advanced NSCLC. This is potentially a supplementary biomarker to TPS as determined by a pathologist.

INTRODUCTION

Immuno-oncology (IO) is effective in multiple cancer types, and immune checkpoint inhibitors (ICI) have been approved in more than 15 types of cancer.[1] The only approved companion diagnostic test for ICI in non–small-cell lung carcinoma (NSCLC) is programmed death ligand-1 (PD-L1) expression measured by immunohistochemistry (IHC).[2] Pembrolizumab is superior to standard chemotherapy in terms of tumor response rate (TRR) and survival in patients with tumor proportion score (TPS) $\geq 50\%$[3]; however, treatment outcomes were similar between pembrolizumab and chemotherapy in

patients with PD-L1 TPS 1%-49%.[4] Therefore, development of a novel biomarker to predict ICI response in the clinical setting in patients with metastatic NSCLC with PD-L1 TPS 1%-49% is highly warranted.

Apart from PD-L1 TPS, other immune biomarkers have limited clinical application.[5-7] In theory, tumor-infiltrating lymphocytes (TIL) are the main activator of antitumor immunity and could be a promising biomarker if TIL can be objectively assessed throughout the whole tumor microenvironment (TME). TIL quantification is labor-intensive and limited by spatial distribution in whole-slide images (WSI) and

CONTEXT

Key Objective

Immune checkpoint inhibitors (ICI) are a standard therapy for advanced non–small-cell lung cancer with positive programmed death ligand-1 expression. However, outcomes may vary depending on the patient's tumor microenvironment and there currently is no standard biomarker addressing the tumor microenvironment. Tumor-infiltrating lymphocytes (TIL) are promising biomarkers for predicting treatment outcomes with ICI, but their current application through manual quantification across whole-slide images (WSI) limits their utility, objectivity, and reproducibility in routine practice.

Knowledge Generated

This proof-of-concept study shows that an artificial intelligence–powered spatial TIL analyzer (Lunit SCOPE IO) can segment and quantify multiple histologic components from WSI, and that the identified immune phenotypes correlate with ICI treatment outcomes.

Relevance

An artificial intelligence–powered assessment of WSI for TIL biomarkers and immune phenotypes that correlate with ICI response may help to optimize treatment selection in clinical practice. This will be elucidated in future clinical application studies.

interobserver heterogeneity.[8-10] Thus, it is challenging to define a clinically relevant TIL cutoff point.[11] Current concept of immune phenotype (IP) is based on the status of TIL in TME, which includes inflamed (TIL distributed intratumorally), immune-excluded (TIL excluded, out of cancer stroma), and immune-desert (scant TIL in TME).[12,13] Although clinical outcomes with ICI according to IP have been reported,[14] deficiency remains in standardized methodology for classification.

We have developed an artificial intelligence (AI)–powered spatial TIL analyzer (Lunit SCOPE IO) that is capable of segmentation and quantification of multiple histologic components from hematoxylin and eosin (H&E)–stained WSI.[15,16] We hypothesize that objective classification of IP by Lunit SCOPE IO is an efficacious biomarker for prediction of tumor response to ICI in patients with advanced NSCLC.

METHODS

Data Sets

Lunit SCOPE IO was developed with data from $2.8 \times 10^9 \ \mu m^2$ H&E-stained tissue regions and 6.0×10^5 TIL from 3,166 WSI of 25 cancer types, including NSCLC, annotated by board-certified pathologists (Data Supplement, online only). For image-based validation of AI model to segment cancer epithelium (CE) and cancer stroma (CS), as well as to detect TIL in an independent cohort, lung adenocarcinoma (LUAD, n = 461) and lung squamous cell carcinoma (LUSC, n = 462) images from The Cancer Genome Atlas (TCGA), as well as NSCLC primary tumor tissues from Samsung Medical Center (SMC, n = 1,205) and Seoul National University Bundang Hospital (SNUBH, n = 261) were included for the analysis under study protocols reviewed and approved by the local institutional review boards of SMC (2018-06-103) and SNUBH (B-2006/619-307). Segmentation and TIL detection

performance of the AI model was separately validated using 110 samples from TCGA LUAD/LUSC. Annotated results from the consensus of three pathologists were analyzed as ground-truth. In the SMC and SNUBH data sets, clinical outcomes including best overall response and progression-free survival (PFS) of ICI, anti–PD-1, or anti–PD-L1 agents, assessed by RECIST v1.1,[17] were retrospectively reviewed by investigators. All studies were conducted according to guidelines (Declaration of Helsinki) for biomedical research.

Classification of Immune Phenotype by Lunit SCOPE IO

To analyze spatial analysis of heterogeneous TIL distribution in WSI with various sizes, WSI were divided into 1 mm^2-sized grids and the IP of each grid classified on the basis of the proportion of each component. IP was defined as follows[13,14]: inflamed as TIL density in CE area above the threshold (106/mm^2); immune-excluded as TIL density in CE area below the threshold and TIL density in CS area above the threshold (357/mm^2); and immune-desert as both TIL density in CE area and that in CS area below the thresholds. Inflamed score, immune-excluded score, and immune-desert score of WSI were defined by the number of grids annotated to certain IP divided by total analyzed grids in WSI. Representative IP of WSI was defined as inflamed IP if the inflamed score was above 33.3%, or immune-excluded IP if immune-excluded score was above 33.3% and inflamed score was < 33.3%, and immune-desert IP otherwise.

PD-L1 Immunohistochemistry and Multiple Immunohistochemistry

PD-L1 expression was assessed on the basis of the US Food and Drug Administration–approved Dako PD-L1 IHC 22C3 pharmDx kit (Agilent Technologies, Santa Clara, CA). PD-L1 expression (%) was determined using the TPS, which is the percentage of viable tumor cells showing partial or complete membrane staining.[18] Multiplex IHC
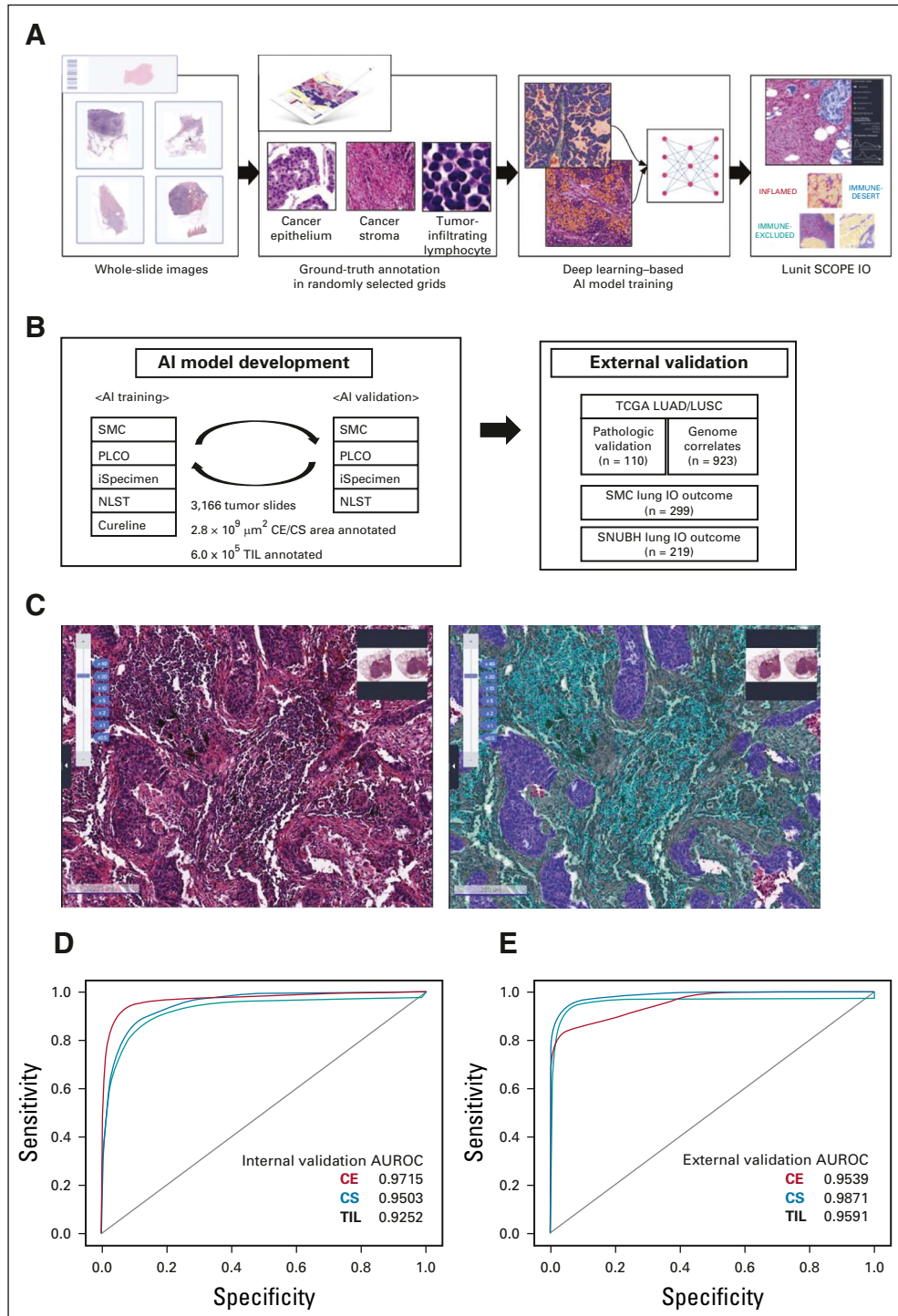
FIG 1. Development of AI-powered tissue analyzer, Lunit SCOPE IO, in non–small-cell lung cancer. (A) The scheme of Lunit SCOPE IO development and the workflow of the current study. (B) Composition of database under Lunit SCOPE IO development. (C) Representative image of H&E original image (left) and Lunit SCOPE IO–inferenced segmentation of CE, purple, CS, green, TIL, cyan, respectively (right). (D) ROC curves to segmentize CE, CS, and to detect TIL in an internal validation cohort. (E) ROC curves to segmentize and detect CE, CS, and to detect TIL, in an external validation cohort (n = 110). The Cancer Genome Atlas lung adenocarcinoma and lung squamous cell carcinoma). AI, artificial intelligence; AUROC, area under the receiver operating characteristic; CE, cancer epithelium; CS, cancer stroma; H&E, hematoxylin and eosin; IP, immune phenotype; LUAD, lung adenocarcinoma; LUSC, lung squamous cell carcinoma; NLST, National Lung Screening Trial; PLCO, Prostate, Lung, Colorectal, and Ovarian Cancer Screening Trial; ROC, receiver operating characteristic; SMC, Samsung Medical Center; SNUBH, Seoul National University Bundang Hospital; TCGA, The Cancer Genome Atlas; TIL, tumor-infiltrating lymphocytes.
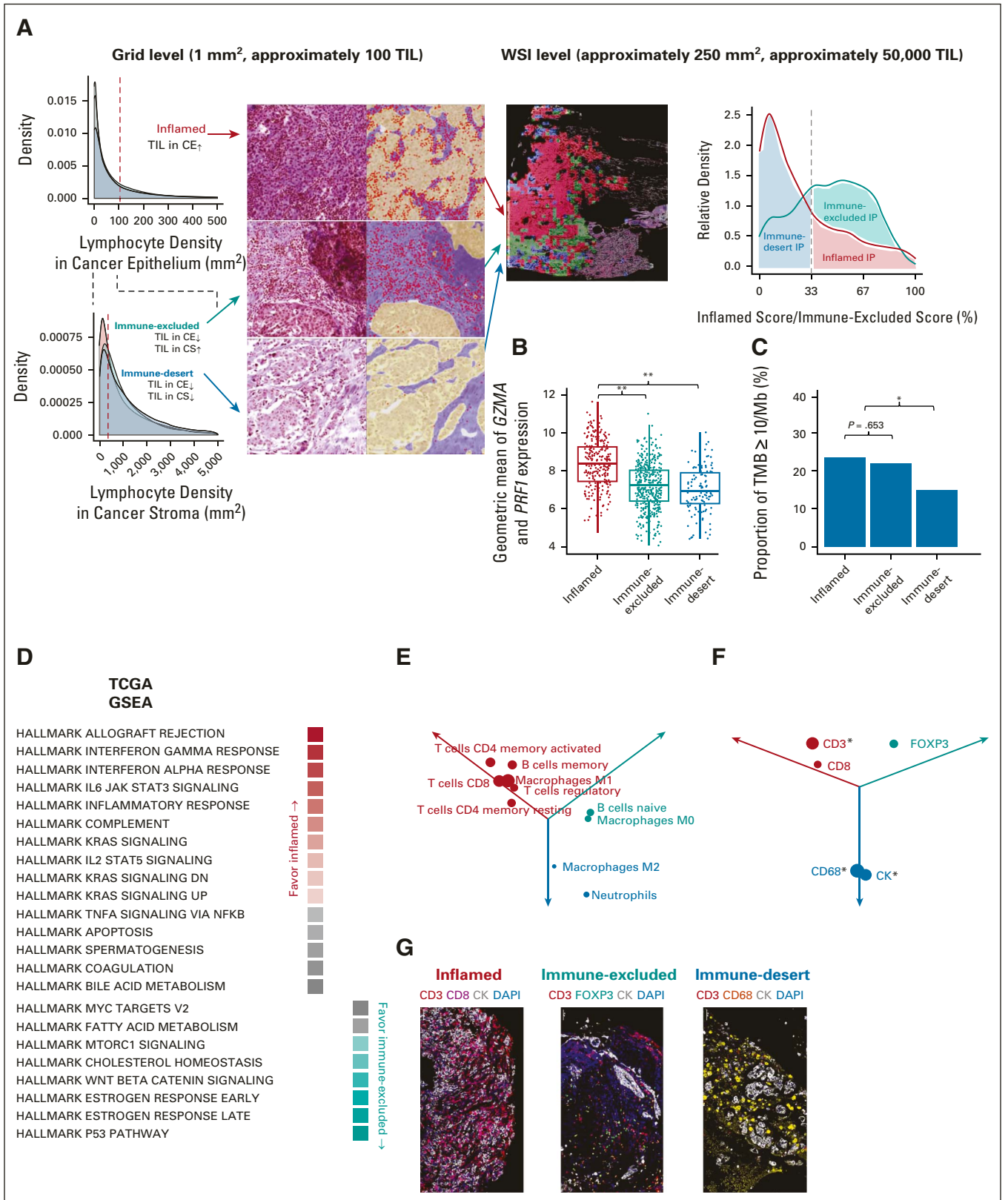
FIG 2. Classification of immune phenotype on the basis of spatial analysis of TIL powered by Lunit SCOPE IO. (A) Distribution of TIL density in CE in TCGA-LUAD and LUSC (WSI n = 923, 1 mm²-sized grid n = 165,646, blue), SMC (WSI n = 1,205, 1 mm²-sized grid n = 121,122, red), and SNUBH (WSI n = 261, 1 mm²-sized grid n = 34,297, teal, top left). Distribution of TIL density in CS in same cohorts (bottom left). Sample H&E images and Lunit SCOPE IO–inferenced masked images of a 1 mm²-sized grid (CE: yellow, CS: purple, and TIL: red) of three immune (continued on following page)

FIG 2. (Continued). phenotypes (middle left). Sample WSI images masked with three immune phenotypes of 1 mm^2-sized grid (inflamed: red, immune-excluded: teal, immune-desert: blue, middle right). Distribution of inflamed score (red) and immune-excluded score (teal) and proportion of representative immune phenotype in TCGA-LUAD and LUSC (right). (B) and (C) Correlation of representative IP (x-axis) and local immune cytolytic activity measured by gene expressions of *GZMA* and *PRF1* (y-axis, B) as well as tumor mutational burden (y-axis, C) in TCGA-LUAD and LUSC. **Represents $P < .001$ and *represents $P < .05$. (D) Summary of ssGSEA using HALLMARK gene sets in TCGA-LUAD and LUSC, filtered by FDR (or q value) < 1%. The mean ratios of ssGSEA scores times –log2 FDR value of inflamed IP or others (red, first column) and those of immune-excluded IP or others (teal, second column). (E) Summary of Cibersort analysis in TCGA-LUAD and LUSC, filtered by P value < .05. Subsets of immune cells enriched in inflamed IP (red), those in immune-excluded IP (teal), and those in immune-desert IP (blue) were annotated. Diameter from zero point to each dot reflected the mean ratio of each IP compared with other IPs times –log2 P value. (F) Summary of multiplex IHC in SMC cohort (n = 99). Quantification of expressing cells was normalized by number of DAPI-stained cells. The normalized count of each expressing cells enriched in inflamed IP (red), that in immune-excluded IP (teal), and that in immune-desert IP (blue) was annotated. Diameter from zero point to each dot reflected the mean ratio of each IP compared with other IPs times –log2 P value. *Represents $P < .05$. (G) Representative multiplex IHC images of inflamed IP (left), immune-excluded IP (middle), and immune-desert IP (right). AI, artificial intelligence; AUROC, area under the receiver operating characteristic; CE, cancer epithelium; CS, cancer stroma; FDR, false discovery rate; H&E, hematoxylin and eosin; IHC, immunohistochemistry; IP, immune phenotype; LUAD, lung adenocarcinoma; LUSC, lung squamous cell carcinoma; SMC, Samsung Medical Center; SNUBH, Seoul National University Bundang Hospital; ssGSEA, single-sample gene set enrichment analysis; TCGA, The Cancer Genome Atlas; TIL, tumor-infiltrating lymphocytes; TMB, tumor mutational burden; WSI, whole-slide image.

was performed per the manufacturers' protocol (Data Supplement). PD-L1 IHC was read by investigators H.K. and Y.-L.C.

Statistical Analysis

Receiver operating characteristic curves and area under the receiver operating characteristics (AUROC) were used to evaluate the AI models. The Kaplan-Meier method was used to estimate PFS or overall survival (OS). Hazard ratios (HR) and 95% CIs were computed using the Cox proportional hazards model, and log-rank test was used to assess differences between groups in PFS or OS. Categorical variables between two groups were compared using the Fisher's exact test, and P values were two-sided. Differences in means or medians for a continuous variable between two groups were assessed by using the nonparametric Mann-Whitney U test. An ensemble of multiple biomarkers to predict ICI responders was established by multivariable logistic regression analysis.

RESULTS

Artificial Intelligence–Powered Tissue Analyzer of Cancer Cell Segmentation and TIL in the TME to Classify Immune Phenotype

Overall, a 2.8×10^9 μm^2 area of CE or CS and 6.0×10^5 TIL was used to develop Lunit SCOPE IO (Figs 1A-1C, Data Supplement). The AUROC for segmentizing CE, CS, and identification of TIL in the internal validation set was 0.9715, 0.9503, and 0.9252, respectively (Fig 1D), and external pathologic validation AUROC was at 0.9539, 0.9871, and 0.9591, respectively (Fig 1E). Moreover, tumor purity estimate and TIL density published previously[19,20] were significantly correlated with those derived from Lunit SCOPE IO in the TCGA LUAD/LUSC cohort (n = 110, Spearman rho = 0.321 and 0.701, $P < .001$; Data Supplement). Because the AI model has been trained on normal lymphoid follicles and macrophage cells as background, Lunit SCOPE IO could discriminate lymphoid

follicles from CE or CS, and macrophage cells from TIL (Data Supplement).

Samples were classified into three IPs by spatial analysis of TIL distribution (Data Supplement). The proportion of grids classified as inflamed, immune-excluded, and desert IP was, respectively, 24.8%, 49.5%, and 25.6% for the TCGA cohort; 30.8%, 37.4%, and 31.8% for the SMC cohort; and 25.0%, 40.1%, and 34.9% for SNUBH cohort (Fig 2A, Data Supplement); distributions were similar between the cohorts.

Immune Phenotype Correlated with Cytolytic Immune Activity and Tumor Mutational Burden

The geometric mean value of gene expressions of *GZMA* and *PRF1* was significantly increased in inflamed IP samples compared with the immune-excluded/ immune-desert IP samples ($P < .001$; Fig 2B). Similar observations were made on the proportion of tumor samples with high tumor mutational burden (TMB; > 10 mutations per megabase),[21,22] with 23.9% and 22.4% in inflamed IP and immune-excluded IP, respectively, but 15.1% in samples with immune-desert IP ($P < .05$, Fig 2C).

Gene set enrichment analysis from TCGA LUAD/LUSC showed that interferon-γ and IL6-STAT3 were highly enriched in inflamed IP, whereas P53 pathway and WNT-β-catenin signaling were more enriched in immune-excluded IP (Fig 2D). The composition of immune cells in the TME calculated by the Cibersort algorithm showed CD8-positive T cells, memory T cells, memory B cells, and M1 macrophages were enriched in inflamed IP, whereas naive B cells and M0 macrophages were enriched in immune-excluded IP.[23] Neutrophils and M2 macrophages were relatively enriched in immune-desert IP (Fig 2E). The multiplex IHC data set from SMC (n = 99) showed a distinct proportion of immune cells according to IP, which demonstrated enrichment of CD3-expressing or CD8-expressing cells in inflamed IP, FOXP3-expressing cells in immune-excluded IP, and CD68-positive cells in immune-desert IP (Figs 2F and 2G).

TABLE 1. Patient Characteristics

Characteristic	All (N = 518)	SMC Cohort (n = 299)	SNUBH Cohort (n = 219)
Age, years, median (range)	65 (33-94)	63 (33-83)	69 (35-94)
Sex, No. (%)			
Female	125 (24.1)	75 (25.1)	50 (22.8)
Male	393 (75.9)	224 (74.9)	169 (77.2)
ECOG PS, No. (%)			
0	26 (5.0)	17 (5.7)	9 (4.1)
1	415 (80.1)	237 (79.3)	178 (81.3)
2	77 (14.9)	45 (15.1)	32 (14.6)
Smoking history, No. (%)			
Never	147 (28.4)	86 (28.8)	61 (27.9)
Former	195 (37.6)	102 (34.1)	93 (42.5)
Current	176 (34.0)	111 (37.1)	65 (29.7)
ICI agent, No. (%)			
Pembrolizumab	229 (44.2)	152 (50.8)	77 (35.2)
Nivolumab	198 (38.2)	108 (36.1)	90 (41.1)
Atezolizumab	80 (15.4)	28 (9.4)	52 (23.7)
Others	11 (2.1)	11 (3.7)	0 (0)
Treatment line, No. (%)			
First-line	43 (8.3)	28 (9.4)	15 (6.8)
Second-line	264 (51.0)	159 (53.2)	105 (47.9)
≥ Third-line	211 (40.7)	112 (37.5)	99 (45.2)
Tissue harvest, No. (%)			
Surgery	160 (30.9)	101 (33.8)	59 (26.9)
Biopsy	358 (69.1)	198 (66.2)	160 (73.1)
Tissue site, No. (%)			
Primary lung	470 (90.7)	251 (83.9)	219 (100)
Pleura	48 (9.3)	48 (16.1)	0 (0)
Pathology, No. (%)			
Adenocarcinoma	296 (57.1)	176 (58.9)	120 (54.8)
Squamous cell carcinoma	158 (30.5)	102 (34.1)	56 (25.6)
Others	64 (12.4)	21 (7.0)	43 (19.6)
Molecular subtype, No. (%)			
EGFR mutation	77 (14.9)	39 (13.0)	38 (17.4)
ALK translocation	6 (1.2)	4 (1.3)	2 (0.9)
EGFR/ALK-negative	406 (78.4)	234 (78.3)	172 (78.5)
Unknown	29 (5.6)	22 (7.4)	7 (3.2)
Liver metastasis at tissue harvest, No. (%)			
No	497 (95.9)	287 (96.0)	210 (95.9)
Yes	21 (4.1)	12 (4.0)	9 (4.1)
Liver metastasis at ICI treatment, No. (%)			
No	453 (87.5)	266 (89.0)	187 (85.4)
Yes	65 (12.5)	33 (11.0)	32 (14.6)

TABLE 1. Patient Characteristics (continued)

Characteristic	All (N = 518)	SMC Cohort (n = 299)	SNUBH Cohort (n = 219)
Pleural metastasis at tissue harvest, No. (%)			
No	381 (73.6)	231 (77.3)	150 (68.5)
Yes	137 (26.4)	68 (22.7)	69 (31.5)
Pleural metastasis at ICI treatment, No. (%)			
No	346 (66.8)	206 (68.9)	140 (63.9)
Yes	172 (33.2)	93 (31.1)	79 (36.1)
Brain metastasis at tissue harvest			
No	446 (86.1)	268 (89.6)	178 (81.3)
Yes	72 (13.9)	31 (10.4)	41 (18.7)
Brain metastasis at ICI treatment, No. (%)			
No	399 (77.0)	242 (80.9)	157 (71.7)
Yes	119 (23.0)	57 (19.1)	62 (28.3)
Time from tissue harvest to ICI treatment, No. (%)			
< 1 year	320 (61.8)	171 (57.2)	149 (68.0)
≥ 1 year	198 (38.2)	128 (42.8)	70 (32.0)
PD-L1 TPS,[a] No. (%)			
0%	104 (23.4)	52 (21.6)	52 (25.6)
1%-49%	134 (30.2)	73 (30.3)	61 (30.0)
≥ 50%	206 (46.4)	116 (48.1)	90 (44.3)

Abbreviations: ALK, anaplastic lymphoma kinase; ECOG PS, Eastern Cooperative Oncology Group performance status; EGFR, epidermal growth factor receptor; ICI, immune checkpoint inhibitor; PD-L1, programmed death ligand-1; SMC, Samsung Medical Center; SNUBH, Seoul National University Bundang Hospital; TPS, tumor proportion score.

[a]PD-L1 status was not assessed in n = 58 from SMC and n = 16 from SNUBH.

Immune Phenotype and Clinical Outcome of Immune Checkpoint Inhibitors

To validate IP as a complementary biomarker in NSCLC, we retrospectively analyzed patients with advanced NSCLC who were treated with ICI monotherapy at either SMC (n = 299) or SNUBH (n = 219). Overall, 518 of 552 eligible patients fulfilled the tissue quality criteria (Data Supplement). In the samples used in this study, ICI had been administered as first-, second-, or ≥ third-line therapy. Clinical characteristics of these two patient cohorts are summarized in Table 1, with minor differences between the two cohorts. Most patients received ICI as second- or ≥ third-line therapy, and more patients received third-line therapy or beyond in the SNUBH cohort (45.2%). Distribution of PD-L1 TPS status was similar; however, the proportion of patients with PD-L1 TPS ≥ 50% (48.1% and 44.3% for SMC and SNUBH, respectively) appeared to be more prevalent than reported in historic data (23.2%-28.5%).[24,25] Distribution of IP by baseline clinical attributes and smoking history was investigated, and there was no correlation between IP and smoking status, liver metastasis, and lung immune prognostic index score[26]; however, some correlation existed between IP and pleural effusion and brain metastasis at the point of tissue harvest (Data Supplement).

Distribution of inflamed, immune-excluded, and immune-desert IP in the SMC cohort was 42.1%, 37.8%, and 20.1%, respectively, and 46.6%, 36.1%, and 17.4%, in the SNUBH cohort (Fig 3A). Incidence of inflamed IP correlated significantly with PD-L1 TPS ≥ 50% status in both cohorts. In a merged cohort of SMC and SNUBH, the overall response rate to ICI in patients with inflamed IP was 26.8%, compared with 11.5% and 11.2% in patients with immune-excluded and immune-desert IP, respectively (odds ratio, 2.84; $P < .001$). Median PFS with ICI among the inflamed, immune-excluded, and immune-desert IP in the merged cohort was 4.1, 2.2, and 2.4 months, respectively (HR 1.52, $P < .001$ for immune-excluded v inflamed IP and 1.58, $P < .001$ for immune-desert IP v inflamed IP; Fig 3B). Improvement in OS after ICI treatment was observed in patients with inflamed IP, and median OS with ICI among the inflamed, immune-excluded, and immune-desert IP in the merged cohort was 24.8, 14.0, and 10.6 months, respectively (HR = 1.38, $P < .05$ for immune-excluded v inflamed IP and 1.67, $P < .05$ for immune-desert IP v inflamed IP). A subgroup analysis of the SMC and SNUBH cohorts showed that each population followed similar trends to the merged cohort (Data Supplement).

To clarify whether IP is a general prognostic marker in NSCLC or a specific predictive biomarker of ICI treatment, we analyzed treatment outcome of first-line platinum-based chemotherapy (n = 373) in the same data set, excluding
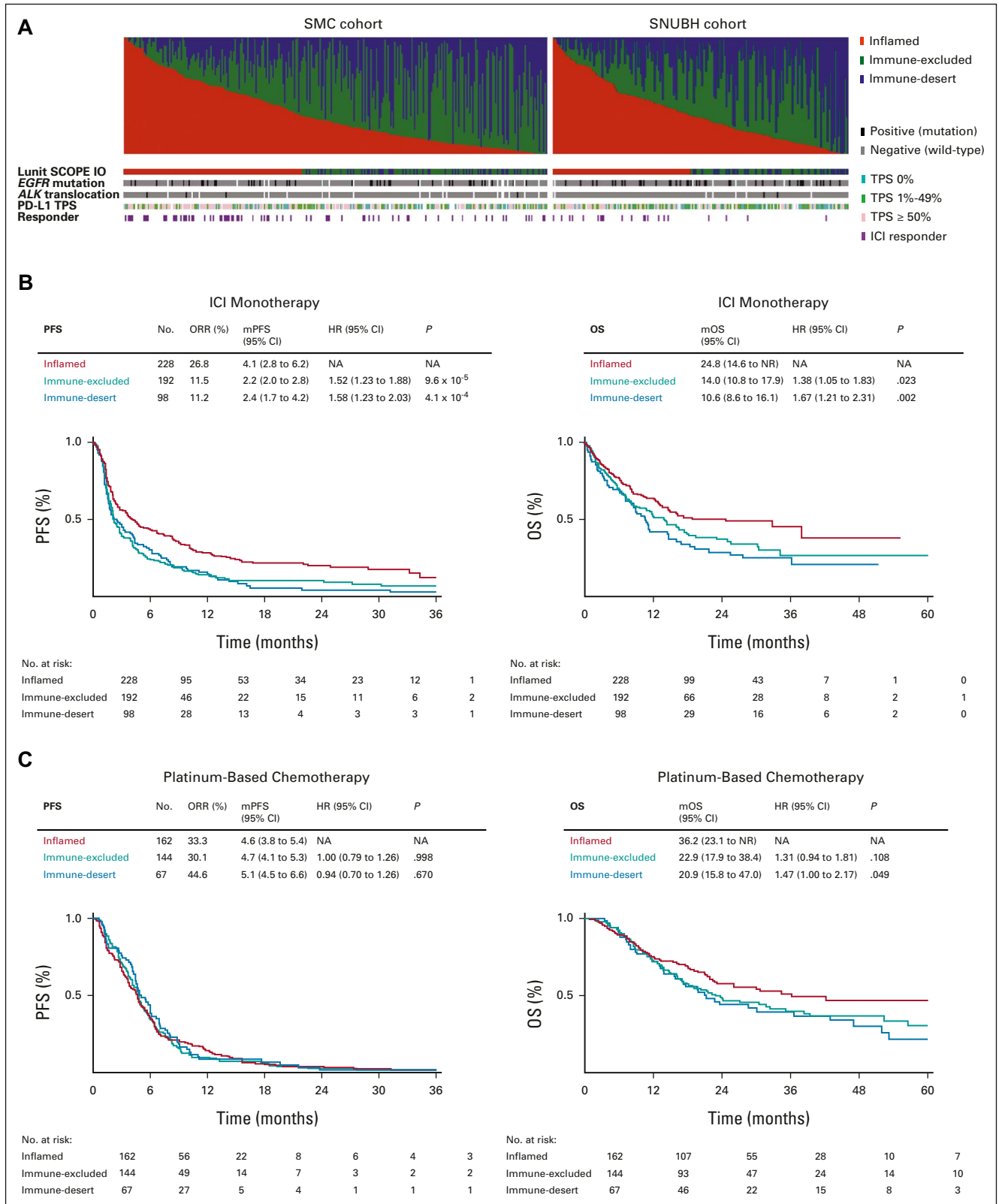
FIG 3. Landscape and clinical significance of Lunit SCOPE IO–powered immune phenotype. (A) Proportion of inflamed score (red), immune-excluded score (green), and immune-desert score (blue, first row), representative IP (second row), *EGFR* mutation status, *ALK* translocation status (black: positive, gray: negative, and blank: unknown), PD-L1 immunohistochemistry TPS (pink: ≥ 50%, green: 1%-49%, and teal: 0%), and best overall response by RECIST v1.1 (purple: complete response or partial response, and blank: stable disease or progressive disease) of each patient were shown (left: SMC, right: SNUBH). (B) Kaplan-Meier analysis of progression-free survival (left) and overall survival after ICI treatment (right) on (continued on following page)

FIG 3. (Continued). the basis of representative immune phenotype in the merged cohort from SMC and SNUBH. (C) Kaplan-Meier analysis of PFS (left) and OS after first-line platinum-based chemotherapy (right) on the basis of representative immune phenotype in a merged cohort. ALK, anaplastic lymphoma kinase; EGFR, epidermal growth factor receptor; HR, hazard ratio; ICI, immune checkpoint inhibitor; IP, immune phenotype; mOS, median overall survival; mPFS, median progression-free survival; NA, not applicable; NR, not reported; ORR, overall response rate; OS, overall survival; PD-L1, programmed death ligand-1; PFS, progression-free survival; SMC, Samsung Medical Center; SNUBH, Seoul National University Bundang Hospital; TPS, tumor proportion score.

the patients who treated ICI as first-line (n = 43), epidermal growth factor receptor (*EGFR*) mutation or anaplastic lymphoma kinase (*ALK*) translocation (n = 83, one duplicated *ALK*+ patient was treated with ICI as first-line), and outside referral (n = 20). PFS and overall response rate of first-line platinum-based chemotherapy were not significantly different according to IP (Fig 3C), but median OS after first-line platinum-based chemotherapy in patients with inflamed, immune-excluded, and immune-desert IP in this cohort was 36.2, 22.9, and 20.9 months, respectively.

In the 43 patients who received first-line ICI and who had an inflamed IP, compared with noninflamed, median PFS was significantly greater (15.6 months *v* 4.8 months; HR, 0.42; 95% CI, 0.19 to 0.90; *P* = .022) and median OS was numerically greater (38.0 months *v* 11.9 months; HR, 0.53; 95% CI, 0.22 to 1.28; *P* = .1483; Data Supplement).

Immune Phenotype in Relation to PD-L1 TPS Status

A combined cohort (Fig 4A; Data Supplement) was used to explore the relationship between IP and PD-L1 TPS status. Incidence of inflamed IP in patients with PD-L1 TPS at < 1%, 1%-49%, and ≥ 50% was 31.7%, 42.5%, and 56.8%, respectively (Fig 4B). By contrast, the incidence of immune-desert IP was more common in the PD-L1 TPS < 1% subgroup (25.0%) compared with the PD-L1 TPS 1%-49% (17.9%) and > 50% (15.0%) subgroups. PD-L1 TPS status correlated well with inflamed IP. TRR of patients with inflamed IP and PD-L1 TPS at < 1%, 1%-49%, and ≥ 50% was 3.0%, 22.8%, and 36.8%, respectively, whereas TRR for patients with noninflamed IP and PD-L1 TPS at < 1%, 1%-49%, and ≥ 50% was 5.6%, 3.9%, and 20.2%, respectively. Median PFS for the inflamed and noninflamed IP was 4.0 versus 2.1 months (HR, 0.54; 95% CI 0.37 to 0.79; *P* = .001) for the PD-L1 TPS 1%-49% subgroup, and 6.2 versus 3.2 months (HR, 0.63; 95% CI, 0.46 to 0.87; *P* = .004) for the PD-L1 TPS ≥ 50% subgroup (Fig 4C); there was no significant difference in OS between IP subgroups (Data Supplement). In the PD-L1 TPS 1%-49% subgroup, the AUROC for prediction of tumor response to ICI by IP was 0.7609, and the AUROC by PD-L1 TPS status was 0.5561 (*P* < .05; Fig 4D). Incidence of inflamed IP was not related to *EGFR* mutation, and there was correlation between inflamed IP score and PD-L1 TPS status in patients either with *EGFR* mutation or those who were *EGFR*/*ALK* wild-type (Data Supplement). Patients with *ALK* translocation were excluded because of a small sample size.

DISCUSSION

In this proof-of-concept study, the AI-powered spatial TIL analyzer was capable of predicting clinical outcomes of ICI in patients with advanced NSCLC. By training and validating the AI-powered spatial TIL analyzer, we have correlated three IPs with local immune cytolytic activities. On the basis of two external independent cohorts of mostly previously treated patients who received monotherapy ICI, we have shown that patients with inflamed IP correlated with higher TRR and longer PFS. A prior retrospective study on manual quantification of TIL reported favorable PFS from ICI treatment in patients with high TIL infiltrate (n = 221; HR 0.40).[27] To our knowledge, ours is the first study on AI-powered automated TIL analysis in advanced NSCLC.

We used a supervised learning model using original images with independent annotated marking of CE, CS, and TIL as assessed by a panel of experienced pathologists, improving on earlier versions of AI technology[28,29]; this meticulous supervision enabled pixel-based spatial analysis of TIL in reference to CE or CS, which is essential for objective quantification and eventual classification of IP. The International TILs Working Group defined the stromal TIL cutoff at > 10%, which is estimated to be about 318/mm², and this also correlates with the clinical outcome of ICI in NSCLC.[29] For urothelial cancer, Mariathasan et al[14] used TIL < 10 per ×200 field as the cutoff level for immune-desert phenotype, but there was no objective cutoff for the inflamed or excluded phenotype. There was no prior objective classification on IP in WSI, which is about 100 times larger than focal area. We applied intratumoral TIL > 106/mm² and stromal TIL > 357 mm² on the basis of upper 25% and lower 25% values from TCGA database in focal area sized 1 mm², and we have defined the representative IP in WSI to be inflamed when more than 33.3% of the grids are read as inflamed. This may be perceived as tentative, but this is an important first step for quantitative classification of IP by AI. The classification is also supported by evidence of higher TMB and gene expressions of *GZMA* and *PRF1*.

Subgroup analysis of KEYNOTE 042 reported the TRR of single agent pembrolizumab in patients with PD-L1 TPS 1%-49% at 17% in treatment-naive patients,[4] suggesting that selected patients can benefit from ICI alone. This AI-powered spatial TIL analyzer may potentially supplement PD-L1 TPS as a supporting biomarker for ICI. In the combined cohort, 42.5% of patients with PD-L1 1%-49% were classified as having inflamed IP, and the TRR was 22.8% in the predominantly pretreated patients compared with a response rate of 3.9% in patients with PD-L1 1%-49% and noninflamed IP. Corresponding to this, the observed median PFS for the inflamed IP was 4.0 months and for noninflamed IP was 2.1 months (*P* = .0013). The
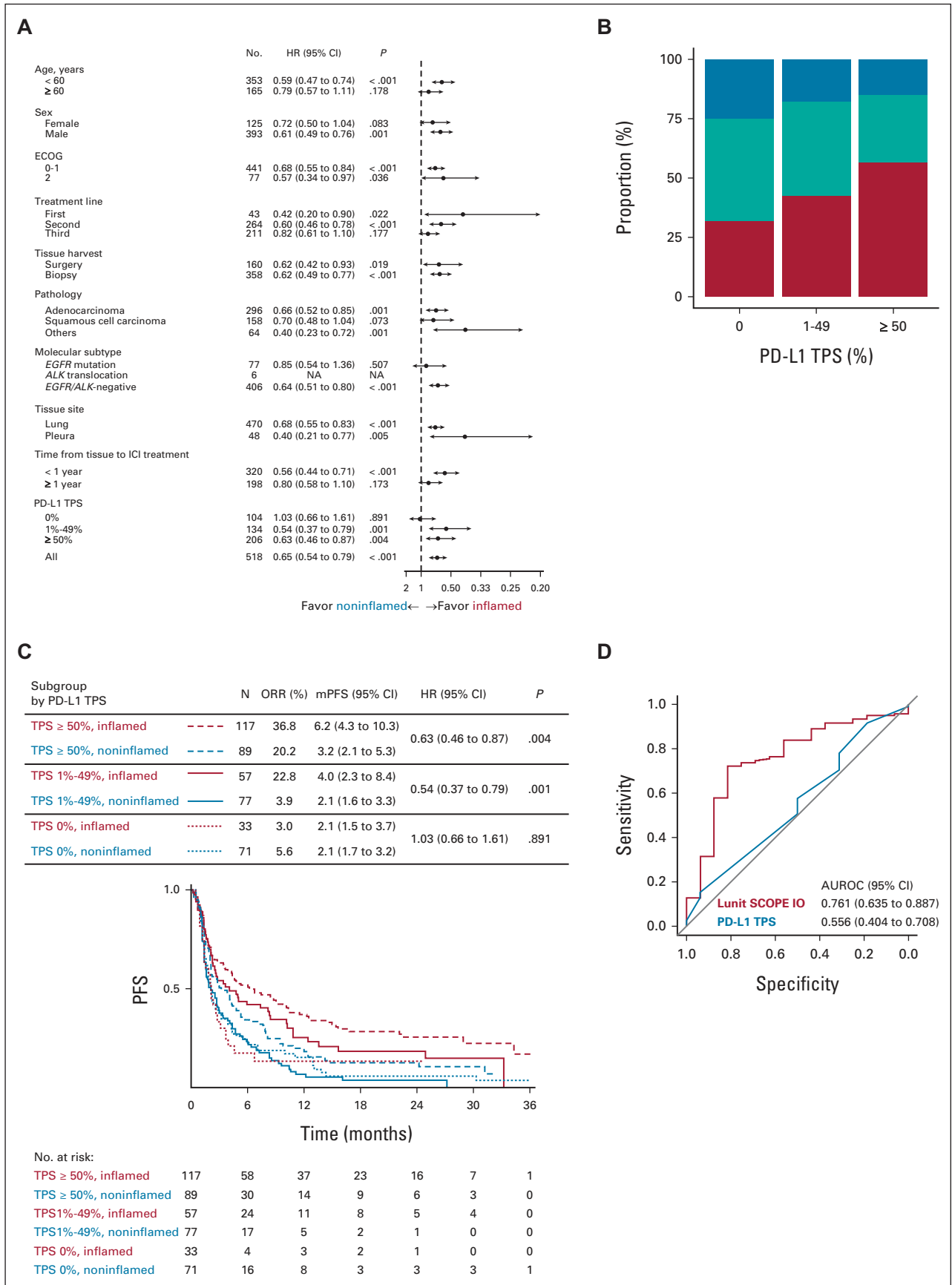
A

	No.	HR (95% CI)	P
Age, years			
< 60	353	0.59 (0.47 to 0.74)	< .001
≥ 60	165	0.79 (0.57 to 1.11)	.178
Sex			
Female	125	0.72 (0.50 to 1.04)	.083
Male	393	0.61 (0.49 to 0.76)	.001
ECOG			
0-1	441	0.68 (0.55 to 0.84)	< .001
2	77	0.57 (0.34 to 0.97)	.036
Treatment line			
First	43	0.42 (0.20 to 0.90)	.022
Second	264	0.60 (0.46 to 0.78)	< .001
Third	211	0.82 (0.61 to 1.10)	.177
Tissue harvest			
Surgery	160	0.62 (0.42 to 0.93)	.019
Biopsy	358	0.62 (0.49 to 0.77)	< .001
Pathology			
Adenocarcinoma	296	0.66 (0.52 to 0.85)	.001
Squamous cell carcinoma	158	0.70 (0.48 to 1.04)	.073
Others	64	0.40 (0.23 to 0.72)	.001
Molecular subtype			
EGFR mutation	77	0.85 (0.54 to 1.36)	.507
ALK translocation	6	NA	NA
EGFR/ALK-negative	406	0.64 (0.51 to 0.80)	< .001
Tissue site			
Lung	470	0.68 (0.55 to 0.83)	< .001
Pleura	48	0.40 (0.21 to 0.77)	.005
Time from tissue to ICI treatment			
< 1 year	320	0.56 (0.44 to 0.71)	< .001
≥ 1 year	198	0.80 (0.58 to 1.10)	.173
PD-L1 TPS			
0%	104	1.03 (0.66 to 1.61)	.891
1%-49%	134	0.54 (0.37 to 0.79)	.001
≥ 50%	206	0.63 (0.46 to 0.87)	.004
All	518	0.65 (0.54 to 0.79)	< .001

Favor noninflamed← →Favor inflamed

B

C

Subgroup by PD-L1 TPS		N	ORR (%)	mPFS (95% CI)	HR (95% CI)	P
TPS ≥ 50%, inflamed	- - -	117	36.8	6.2 (4.3 to 10.3)	0.63 (0.46 to 0.87)	.004
TPS ≥ 50%, noninflamed	- - -	89	20.2	3.2 (2.1 to 5.3)		
TPS 1%-49%, inflamed	———	57	22.8	4.0 (2.3 to 8.4)	0.54 (0.37 to 0.79)	.001
TPS 1%-49%, noninflamed	———	77	3.9	2.1 (1.6 to 3.3)		
TPS 0%, inflamed	······	33	3.0	2.1 (1.5 to 3.7)	1.03 (0.66 to 1.61)	.891
TPS 0%, noninflamed	······	71	5.6	2.1 (1.7 to 3.2)		

No. at risk:

TPS ≥ 50%, inflamed	117	58	37	23	16	7	1
TPS ≥ 50%, noninflamed	89	30	14	9	6	3	0
TPS1%-49%, inflamed	57	24	11	8	5	4	0
TPS1%-49%, noninflamed	77	17	5	2	1	0	0
TPS 0%, inflamed	33	4	3	2	1	0	0
TPS 0%, noninflamed	71	16	8	3	3	3	1

D

	AUROC (95% CI)
Lunit SCOPE IO	0.761 (0.635 to 0.887)
PD-L1 TPS	0.556 (0.404 to 0.708)

FIG 4. Lunit SCOPE IO–powered immune phenotype dictates the responder of immune checkpoint inhibitors especially in PD-L1 tumor proportion score 1%-49%. (A) Forest plot of HR (dot) and 95% CI (arrow) for PFS according to each clinicopathologic subgroup. (B) (continued on following page)

majority of these patients received ICI as second- or ≥ third-line therapy. Our finding in this enriched population appears to be superior to the reported response rate of 14.8% of the PD-L1 1%-49% subgroup from the KEYNOTE 001 study.[24] In the small subset of patients (n = 10) who received first-line ICI, the TRR of patients with inflamed versus non-inflamed IP was 66.7% versus 0%. Despite the small sample size, the result is remarkable compared with the prior randomized study on first-line ICI.[3] IP classified by the AI-powered spatial TIL analyzer is potentially complementary to PD-L1 expression and may help to identify patient with PD-L1 TPS 1%-49% who may benefit from ICI monotherapy.

On the basis of our current cutoff threshold, we can correlate the inflamed IP with higher TRR and longer survival. This may potentially serve as a relatively low-cost and efficient biomarker on the basis of H&E-stained slides from routine clinical practice.

This retrospective study is limited by the intrinsic heterogeneous nature of multiple patient cohorts. This might explain why the difference in survival in the validation cohort (SNUBH) is not significant because there are more patients receiving ICI as third-line therapy (or beyond) than other study cohorts and, overall, there were only 43 patients enrolled who received first-line ICI. The greatest challenge is to define the cutoff threshold for inflamed IP as there is no prior example of quantitative measurement of inflammation status of the TME.

The lag time between biopsy and ICI, and differences in patient demographics between two institutions (SMC and SNUBH) are major limitations to this study. There was diverse opinion among oncologists on the optimal timing in use of ICI, driven by the reimbursement criteria and policies in Korea (Data Supplement), and as a result, exposure to other therapy may affect TME. Because of the retrospective nature of study, significant differences in PD-L1 TPS status and in lines of prior therapy were observed.

Tumor genomic aberration or clinical attributes may affect TIL status or IP of TME. Because of the retrospective nature of the study, we were not able to assess systemic immune status for all patients included in the current study; however, pleural effusion and brain metastasis at tissue harvest were significantly related to IP. A limitation of this analysis was that samples such as lymph node or distant metastasis were not included.

In conclusion, Lunit SCOPE IO can process H&E-stained slides simultaneously with PD-L1 IHC. Patients with inflamed IP have higher TRR and longer PFS with ICI monotherapy, and this development may serve as a complementary biomarker to PD-L1 TPS for advanced NSCLC, especially the PD-L1 TPS 1%-49% subgroup. Future prospective study of the clinical application of Lunit SCOPE IO in treatment of advanced NSCLC is warranted.

AFFILIATIONS

[1]Division of Hematology-Oncology, Department of Medicine, Samsung Medical Center, Sungkyunkwan University School of Medicine, Seoul 06351, Republic of Korea
[2]Lunit, Seoul, Republic of Korea
[3]Department of Pathology, Seoul National University Bundang Hospital, Seongnam, Republic of Korea
[4]Department of Pathology and Translational Genomics, Samsung Medical Center, Sungkyunkwan University School of Medicine, Seoul, Republic of Korea
[5]Department of Pathology, Ajou University School of Medicine, Suwon, Republic of Korea
[6]Division of Hematology-Oncology, Department of Internal Medicine, Seoul National University Bundang Hospital, Seongnam, Republic of Korea
[7]Department of Internal Medicine, Seoul National University College of Medicine, Seoul, Republic of Korea
[8]State Key Laboratory of Translational Oncology, Department of Clinical Oncology, Chinese University of Hong Kong, Hong Kong, China
[9]Department of Health Sciences and Technology, Samsung Advanced Institute of Health Sciences and Technology, Sungkyunkwan University, Seoul, Republic of Korea

CORRESPONDING AUTHOR

Se-Hoon Lee, Division of Hematology-Oncology, Department of Medicine, Samsung Medical Center, Sungkyunkwan University School of Medicine, Seoul 06351, Republic of Korea; e-mail: shlee119@skku.edu.

EQUAL CONTRIBUTION

S.P., C.-Y.O., and H.K. contributed equally to this work. Y.-L.C., T.S.M., and S.-H.L. contributed equally to this study as co-senior authors.

AUTHORS' DISCLOSURES OF POTENTIAL CONFLICTS OF INTEREST

Disclosures provided by the authors are available with this article at DOI https://doi.org/10.1200/JCO.21.02010.

AUTHOR CONTRIBUTIONS

Conception and design: Sehhoon Park, Chan-Young Ock, Hyojin Kim, Sergio Pereira, Kyunghyun Paeng, Donggeun Yoo, Yoon-La Choi, Tony S. Mok, Se-Hoon Lee
Financial support: Se-Hoon Lee
Administrative support: Tony S. Mok, Se-Hoon Lee
Provision of study materials or patients: Sehhoon Park, Chan-Young Ock, Hyojin Kim, Koung Jin Suh, Hyun Ae Jung, Se Hyun Kim, Yu Jung Kim, Jong-Mu Sun, Jin-Haeng Chung, Jin Seok Ahn, Myung-Ju Ahn, Jong Seok Lee, Keunchil Park, Yoon-La Choi, Se-Hoon Lee
Collection and assembly of data: Sehhoon Park, Chan-Young Ock, Hyojin Kim, Sergio Pereira, Sangjoon Choi, Seokhwi Kim, Seunghwan Shin,

Brian Jaehong Aum, Donggeun Yoo, Hongui Cha, Sunyoung Park, Koung Jin Suh, Hyun Ae Jung, Se Hyun Kim, Yu Jung Kim, Jong-Mu Sun, Jin-Haeng Chung, Jin Seok Ahn, Jong Seok Lee, Sang Yong Song, Se-Hoon Lee
Data analysis and interpretation: Sehhoon Park, Chan-Young Ock, Seonwook Park, Minuk Ma, Seokhwi Kim, Donggeun Yoo, Jin Seok Ahn, Myung-Ju Ahn, Keunchil Park, Yung-Jue Bang, Yoon-La Choi, Tony S. Mok, Se-Hoon Lee
Manuscript writing: All authors
Final approval of manuscript: All authors
Accountable for all aspects of the work: All authors

ACKNOWLEDGMENT

REFERENCES

1. Pan C, Liu H, Robins E, et al: Next-generation immuno-oncology agents: Current momentum shifts in cancer immunotherapy. J Hematol Oncol 13:29, 2020
2. US Food and Drug Administration: PD-L1 IHC 22C3 pharmDx—P150013/S014, 2020 https://www.accessdata.fda.gov/scripts/cdrh/cfdocs/cfpma/pma.cfm?id=P150013S014
3. Reck M, Rodriguez-Abreu D, Robinson AG, et al: Pembrolizumab versus chemotherapy for PD-L1-positive non-small-cell lung cancer. N Engl J Med 375:1823-1833, 2016
4. Mok TSK, Wu YL, Kudaba I, et al: Pembrolizumab versus chemotherapy for previously untreated, PD-L1-expressing, locally advanced or metastatic non-small-cell lung cancer (KEYNOTE-042): A randomised, open-label, controlled, phase 3 trial. Lancet 393:1819-1830, 2019
5. Ayers M, Lunceford J, Nebozhyn M, et al: IFN-gamma-related mRNA profile predicts clinical response to PD-1 blockade. J Clin Invest 127:2930-2940, 2017
6. Zito Marino F, Ascierto PA, Rossi G, et al: Are tumor-infiltrating lymphocytes protagonists or background actors in patient selection for cancer immunotherapy? Expert Opin Biol Ther 17:735-746, 2017
7. Arora S, Velichinskii R, Lesh RW, et al: Existing and emerging biomarkers for immune checkpoint immunotherapy in solid tumors. Adv Ther 36:2638-2678, 2019
8. Khoury T, Peng X, Yan L, et al: Tumor-infiltrating lymphocytes in breast cancer: Evaluating interobserver variability, heterogeneity, and fidelity of scoring core biopsies. Am J Clin Pathol 150:441-450, 2018
9. Swisher SK, Wu Y, Castaneda CA, et al: Interobserver agreement between pathologists assessing tumor-infiltrating lymphocytes (TILs) in breast cancer using methodology proposed by the International TILs Working Group. Ann Surg Oncol 23:2242-2248, 2016
10. Buisseret L, Desmedt C, Garaud S, et al: Reliability of tumor-infiltrating lymphocyte and tertiary lymphoid structure assessment in human breast cancer. Mod Pathol 30:1204-1212, 2017
11. Gao G, Wang Z, Qu X, et al: Prognostic value of tumor-infiltrating lymphocytes in patients with triple-negative breast cancer: A systematic review and meta-analysis. BMC Cancer 20:179, 2020
12. Joyce JA, Fearon DT: T cell exclusion, immune privilege, and the tumor microenvironment. Science 348:74-80, 2015
13. Chen DS, Mellman I: Elements of cancer immunity and the cancer-immune set point. Nature 541:321-330, 2017
14. Mariathasan S, Turley SJ, Nickles D, et al: TGFbeta attenuates tumour response to PD-L1 blockade by contributing to exclusion of T cells. Nature 554:544-548, 2018
15. Paeng K, Hwang S, Park S, et al: A unified framework for tumor proliferation score prediction in breast histopathology. Lecture Notes in Computer Science (including subseries Lecture Notes in Artificial Intelligence and Lecture Notes in Bioinformatics), 2017
16. Pantanowitz L, Hartman D, Qi Y, et al: Accuracy and efficiency of an artificial intelligence tool when counting breast mitoses. Diagn Pathol 15:80, 2020
17. Eisenhauer EA, Therasse P, Bogaerts J, et al: New response evaluation criteria in solid tumours: Revised RECIST guideline (version 1.1). Eur J Cancer 45:228-247, 2009
18. Roach C, Zhang N, Corigliano E, et al: Development of a companion diagnostic PD-L1 immunohistochemistry assay for pembrolizumab therapy in non-small-cell lung cancer. Appl Immunohistochem Mol Morphol 24:392-397, 2016
19. Aran D, Sirota M, Butte AJ: Systematic pan-cancer analysis of tumour purity. Nat Commun 6:8971, 2015
20. Saltz J, Gupta R, Hou L, et al: Spatial organization and molecular correlation of tumor-infiltrating lymphocytes using deep learning on pathology images. Cell Rep 23:181-193 e7, 2018
21. Hellmann MD, Paz-Ares L, Bernabe Caro R, et al: Nivolumab plus ipilimumab in advanced non-small-cell lung cancer. N Engl J Med 381:2020-2031, 2019
22. Marabelle A, Fakih M, Lopez J, et al: Association of tumour mutational burden with outcomes in patients with advanced solid tumours treated with pembrolizumab: Prospective biomarker analysis of the multicohort, open-label, phase 2 KEYNOTE-158 study. Lancet Oncol 21:1353-1365, 2020
23. Coudray N, Ocampo PS, Sakellaropoulos T, et al: Classification and mutation prediction from non-small cell lung cancer histopathology images using deep learning. Nat Med 24:1559-1567, 2018
24. Garon EB, Rizvi NA, Hui R, et al: Pembrolizumab for the treatment of non-small-cell lung cancer. N Engl J Med 372:2018-2028, 2015

25. Herbst RS, Baas P, Kim DW, et al: Pembrolizumab versus docetaxel for previously treated, PD-L1-positive, advanced non-small-cell lung cancer (KEYNOTE-010): A randomised controlled trial. Lancet 387:1540-1550, 2016

26. Mezquita L, Auclin E, Ferrara R, et al: Association of the lung immune prognostic index with immune checkpoint inhibitor outcomes in patients with advanced non-small cell lung cancer. JAMA Oncol 4:351-357, 2018

27. Gataa I, Mezquita L, Rossoni C, et al: Tumour-infiltrating lymphocyte density is associated with favourable outcome in patients with advanced non-small cell lung cancer treated with immunotherapy. Eur J Cancer 145:221-229, 2021

28. Campanella G, Hanna MG, Geneslaw L, et al: Clinical-grade computational pathology using weakly supervised deep learning on whole slide images. Nat Med 25:1301-1309, 2019

29. Salgado R, Denkert C, Demaria S, et al: The evaluation of tumor-infiltrating lymphocytes (TILs) in breast cancer: Recommendations by an International TILs Working Group 2014. Ann Oncol 26:259-271, 2015

■ ■ ■

ASCO® AMERICAN SOCIETY OF CLINICAL ONCOLOGY
KNOWLEDGE CONQUERS CANCER

ASCO offers premier scientific events for oncology professionals, patient advocates, industry representatives, and major media outlets worldwide.

View upcoming Meetings and Symposia at **meetings.asco.org**.

AUTHORS' DISCLOSURES OF POTENTIAL CONFLICTS OF INTEREST

Artificial Intelligence–Powered Spatial Analysis of Tumor-Infiltrating Lymphocytes as Complementary Biomarker for Immune Checkpoint Inhibition in Non–Small-Cell Lung Cancer

The following represents disclosure information provided by authors of this manuscript. All relationships are considered compensated unless otherwise noted. Relationships are self-held unless noted. I = Immediate Family Member, Inst = My Institution. Relationships may not relate to the subject matter of this manuscript. For more information about ASCO's conflict of interest policy, please refer to www.asco.org/rwc or ascopubs.org/jco/authors/author-center.

Open Payments is a public database containing information reported by companies about payments made to US-licensed physicians (Open Payments).

Sehhoon Park
Stock and Other Ownership Interests: Lunit

Chan-Young Ock
Employment: Lunit
Leadership: Lunit
Stock and Other Ownership Interests: Lunit, Medpacto, Y-Biologics
Consulting or Advisory Role: Medpacto, Y-Biologics, Idience

Sergio Pereira
Employment: Lunit
Stock and Other Ownership Interests: Lunit

Seonwook Park
Employment: Lunit
Stock and Other Ownership Interests: Lunit
Research Funding: Lunit

Minuk Ma
Employment: Lunit
Stock and Other Ownership Interests: Lunit

Seunghwan Shin
Employment: Lunit
Stock and Other Ownership Interests: Lunit

Jaehong Aum
Employment: Lunit
Stock and Other Ownership Interests: Lunit

Kyunghyun Paeng
Employment: Lunit
Leadership: Lunit
Stock and Other Ownership Interests: Lunit

Donggeun Yoo
Employment: Lunit
Leadership: Lunit
Stock and Other Ownership Interests: Lunit
Patents, Royalties, Other Intellectual Property: Having several patents about medical AI developments in Lunit Inc

Se Hyun Kim
Consulting or Advisory Role: Ono Pharmaceutical

Jin Seok Ahn
Honoraria: Pfizer, Roche, BC World, Yuhan, Hanmi, Novartis, JW Pharmaceutical, Amgen, Boehringer Ingelheim
Consulting or Advisory Role: Bixink, Bayer, Yooyoung Pharmaceutical Co Ltd, Pharmbio Korea, Vifor Pharma

Myung-Ju Ahn
Honoraria: AstraZeneca, Lilly, MSD, Takeda
Consulting or Advisory Role: AstraZeneca, Boehringer Ingelheim, Lilly, MSD, Takeda, Alpha Pharmaceutical

Keunchil Park
Consulting or Advisory Role: AstraZeneca, Lilly, Ono Pharmaceutical, Bristol Myers Squibb, MSD, Merck KGaA, AbbVie, Daiichi Sankyo, Boehringer Ingelheim, JNJ, Geinus, IMBdx
Speakers' Bureau: Boehringer Ingelheim
Research Funding: AstraZeneca, MSD Oncology

Sang Yong Song
Employment: AstraZeneca/MedImmune
Leadership: AstraZeneca/MedImmune
Stock and Other Ownership Interests: AstraZeneca/MedImmune

Yung-Jue Bang
Consulting or Advisory Role: BeiGene, Green Cross, Merck Serono, AstraZeneca/MedImmune, Novartis, MSD Oncology, Hanmi, Genentech/Roche, Daiichi Sankyo, Astellas Pharma, Bristol Myers Squibb, Samyang, Alexo Therapeutics
Research Funding: AstraZeneca/MedImmune (Inst), Novartis (Inst), Genentech/Roche (Inst), MSD (Inst), Merck Serono (Inst), Bayer (Inst), GlaxoSmithKline (Inst), Bristol Myers Squibb (Inst), Pfizer (Inst), Lilly (Inst), Ono Pharmaceutical (Inst), Taiho Pharmaceutical (Inst), Takeda (Inst), BeiGene (Inst), Curis (Inst), GC Pharma (Inst), Daiichi Sankyo (Inst), Astellas Pharma (Inst), Genexine (Inst)

Yoon-La Choi
Research Funding: Bayer

Tony S. Mok
Employment: The Chinese University of Hong Kong
Leadership: Sanomics Limited, AstraZeneca, Hutchison China Meditech, Aurora Tele-Oncology Platform, Lunit
Stock and Other Ownership Interests: Sanomics Limited, Hutchison China Meditech, Aurora Tele-Oncology Platform
Honoraria: AstraZeneca, Alpha Biopharma, ACEA Pharmaceutical Research, Amgen, Amoy Diagnostics, BeiGene, Boehringer Ingelheim, Bristol Myers Squibb, Daiichi Sankyo/UCB Japan, Fishawack Facilitate, InMed, Lilly, Merck Sharp & Dohme, Novartis, Origimed, Pfizer, Prime Oncology, Roche, Sanofi Aventis GmbH, Taiho Pharmaceutical, Takeda, Lucence Health Inc, Medscape, P. Permanyer SL, PeerVoice, Physicans' Education Resource, Research to Practice, Shanghai BeBirds Translation & Consulting Co, Liangyihui Network Technology Co., Ltd
Consulting or Advisory Role: AbbVie, ACEA Pharmaceutical Research, Alpha Biopharma, Amgen, Amoy Diagnostics, AstraZeneca, BeiGene, Berry Oncology, Boehringer Ingelheim, Blueprint Medicines, Bristol Myers Squibb, CStone Pharmaceuticals, Curio Science, Daiichi Sankyo/UCB Japan, Eisai, Fishawack Facilitate, Gritstone Oncology, Guardant Health, Hengrui Therapeutics, Ignyta, Incyte, Inivata, IQvia, Lilly, Loxo, Lunit, Merck Serono, Merck Sharp & Dohme, Mirati Therapeutics, Novartis, Pfizer, Puma Biotechnology, Roche, SFJ Pharmaceuticals Group, Takeda, Vertex, Yuhan, Qiming Development (HK) Ltd
Research Funding: AstraZeneca (Inst), Boehringer Ingelheim (Inst), Pfizer (Inst), Novartis (Inst), SFJ Pharmaceuticals Group (Inst), Roche (Inst), Merck Sharp & Dohme (Inst), Bristol Myers Squibb (Inst), Xcovery (Inst), G1 Therapeutics (Inst), Merck Serono (Inst), Takeda (Inst)

Se-Hoon Lee
Honoraria: AstraZeneca/MedImmune, Roche, Bristol Myers Squibb, Merck
Consulting or Advisory Role: AstraZeneca, Bristol Myers Squibb, Roche
Research Funding: Merck
Travel, Accommodations, Expenses: Novartis

No other potential conflicts of interest were reported.